UDP-Galactose 4-Epimerase from *Kluyveromyces fragilis*: Analysis of Its Hysteretic Behavior during Catalysis†

Suprabha Nayar,‡,§ Amrita Brahma,‡ Bhaswati Barat,|| and Debasish Bhattacharyya*

Indian Institute of Chemical Biology, 4, Raja S.C. Mallick Road, Jadavpur, Calcutta 700032, India

Received March 3, 2004; Revised Manuscript Received June 5, 2004

ABSTRACT: UDP-galactose 4-epimerase serves as a prototype model of class II oxidoreductases that use bound NAD as a cofactor. This enzyme from *Kluyveromyces fragilis* is a homodimer with a molecular mass of 75 kDa/subunit. Continuous monitoring of the conversion of UDP-galactose (UDP-gal) to UDP-glucose (UDP-glu) by the epimerase in the presence of the coupling enzyme UDP-glucose dehydrogenase and NAD shows a kinetic lag of up to 80 s before a steady state is reached. The disappearance of the lag follows first-order kinetics ($k = 3.22 \times 10^{-2}$ s^{-1}) at 25 °C at enzyme and substrate concentrations of 1.0 nM and 1 mM, respectively. The observed lag is not due to factors such as insufficient activity of the coupling enzyme, association or dissociation or incomplete recruitment of NAD by epimerase, product activation, etc., but was a true expression of the activity of the prepared enzyme. Dissociation of the bound ligand(s) by heat followed by analysis with reverse-phase HPLC, TLC, UV-absorption spectrometry, mass spectrometry, and NMR showed that in addition to 1.78 mol of NAD/dimer, the epimerase also contains 0.77 mol of 5′-UMP/dimer. The latter is a strong competitive inhibitor. Preincubation of the epimerase with the substrate UDP-gal or UDP-glu replaces the inhibitor and also abolishes the lag, which reappeared after the enzyme was treated with 5′-UMP. The lag was not observed as long as the cells were in the growing phase and galactose in the growth medium was limiting, suggesting that association with 5′-UMP is a late log-phase phenomenon. The stoichiometry and conserved amino acid sequence around the NAD binding site of multimeric class I (classical dehydrogenases) and class II oxidoreductases, as reported in the literature, have been compared. It shows that each subunit is independently capable of being associated with one molecule of NAD, suggestive of two NAD binding sites of epimerase per dimer.

UDP-galactose 4-epimerase (EC 5.3.2.1, hereafter called epimerase) is a ubiquitous and obligatory enzyme of galactose metabolism that reversibly converts UDP-galactose (UDP-gal)[1] to UDP-glucose (UDP-glu). It belongs to a rare class of enzymes which utilize noncovalently but strongly bound NAD as a cofactor (class II oxidoreductases) and not as a cosubstrate like NAD/NADH-dependent classical dehydrogenases (class I oxidoreductases) (*1*−*3*). Its mechanism involves abstraction of a hydride from the C-4 position of the sugar nucleotide by NAD prior to formation of a transient enzyme·NADH·keto-substrate complex. The sugar moiety of this complex in turn rotates 180° and abstracts the same hydride, leading to a stereoselective inversion of the OH group. Though epimerases from different sources differ significantly in size and quaternary structure, they share an identical mechanism of action. It collectively acts as a prototype model of class II oxidoreductases in which a similar type of NAD-mediated mechanism is observed but the specificity varies widely (*3*).

The epimerase from yeast *Kluyveromyces fragilis*[2] is a homodimer with a molecular mass of 75 kDa/subunit. Though cloning and sequencing of its gene are yet to be done, extensive biochemical evidence suggests that the enzyme has one bound NAD^+ per dimer (*1*−*5*) and the cofactor is located at the subunit interface (*6*). The enzymes from *Saccharomyces cerevisiae* and *Kluyveromyces lactis* are less characterized but have been cloned and sequenced (*7*). Among epimerases, the X-ray crystallographic structure of the *Escherichia coli* enzyme was first reported at high

† Research was funded by Department of Science and Technology (DST) grants awarded to D.B. (SP/SO/D-45/93 and SP/SO/D-107/98). A senior research fellowship from DST and a research associateship from the Council of Scientific and Industrial Research (CSIR) supported S.N. at different phases. The national eligibility test of CSIR and a junior research fellowship from DST supported B.B. and A.B., respectively.

* To whom correspondence should be addressed. Fax: +91-33-2473-5197/0284. Phone: 091-033-2473-3491/3493/0492, ext. 164. E-mail: debasish@iicb.res.in.

‡ These authors contributed equally to this publication.

§ Present address: National Metallurgical Laboratory, Burmamines, Jamshedpur 831007, Jharkhand, India.

|| Present address: University of California, Los Angeles, CA 90095.

[1] Abbreviations: ANS, 1-anilino-8-naphthalenesulfonic acid; c-AMP, cyclic AMP; BME, β-mercaptoethanol; clean enzyme, epimerase that was devoid of bound 5′-UMP; 5′-UMP, 5′-uridine monophosphate; UDP, uridine diphosphate; UTP, uridine triphosphate; UDP-gal, UDP-galactose; UDP-glu, UDP-glucose; UDP-man, UDP-mannose; UDP-NAG, UDP *N*-acetylglucosamine; UDP-xyl, UDP-xylose; UDP-GA, UDP-glucuronic acid; epimerase, UDP-galactose 4-epimerase (EC 5.1.3.2); UDP-glu DH, UDP-glucose dehydrogenase (EC 1.1.1.22); 5′-nucleotidase, 5′-ribonucleotide phosphohydrolase (EC 3.1.3.5); PNK, T4 polynucleotide kinase (EC 2.7.1.78).

[2] *K. fragilis* has been renamed as *Kluyveromyces marxianus* var. *marxianus*.

10.1021/bi049569t CCC: $27.50
Published on Web 07/16/2004

resolution (*8*, *9*). Its sequence is strongly homologous with the N-terminal part of the yeast enzyme but is only half its size (homodimer, 39 kDa/subunit). An unexpected finding was the existence of two nucleotide and substrate binding sites per dimer situated in a symmetry-oriented manner away from the subunit interface. This was in contrast to the earlier report of one nucleotide bound per dimer (*1*, *2*). Whether the two "catalytic" sites are functional or have allosteric relation is not known. The bound NAD of both yeast and bacterial enzymes can be reduced to NADH with the concomitant loss of activity by "reductive inhibition" (*10*). Recent developments have witnessed cloning, sequencing, and X-ray crystallographic structure analysis of dimeric human epimerase that requires extraneous NAD for catalysis (*11*). Dimerization of yeast epimerase may originate from the point of view of stability or to satisfy a stringency such as subunit-dependent catalytic sites (*6*). The number of bound NAD molecules, which is related to the number of catalytic sites, has not yet been settled with confidence for the yeast enzyme. Thus, there seems to be room to reconsider the stoichiometry and predict the location of the bound cofactor(s) in yeast epimerase.

The epimerase is routinely assayed using UDP-gal as the substrate, the epimerized product UDP-glu being quantified by the coupling enzyme UDP-glucose DH in the presence of NAD, yielding glucuronic acid (*12*). The reaction follows the normal Michaelis−Menten relation. Further, the time course of conversion of the substrate within the hyperbolic zone of the relation follows a linear propagation for at least 8 min. However, the initial phase of conversion by this enzyme from *K. fragilis* showed a lag, enhancement, or no effect. Herein, we report the analysis of the initial phase of activation of this enzyme and redetermination of the stoichiometry of the bound cofactor(s). A comparison of the stoichiometry of the cofactor and sequence homology of its binding sites among class I and II oxidoreductases have also been presented. It is worth mentioning that the lag in catalysis has never been observed while working with *E. coli* epimerase, which was purified from an overexpression plasmid (*13*, *14*).

EXPERIMENTAL PROCEDURES

Materials. Fine chemicals, e.g., ANS, BME, DEAE-cellulose, D(+)-gal, D(+)-glu, glycylglycine, NAD, NADH, Sephadex G-50, 5′-UMP, UDP, UTP, UDP-gal, UDP-glu, UDP-man, UDP-xyl, UDP-GA, UDP-NAG, and 5′-nucleotidase (5′-ribonucleotide phosphohydrolase, from *Crotalus atrox* venom, grade IV, partially purified), were from Sigma. T4 polynucleotide kinase (10 units/mL, catalog no. MO-201S) was from New England Biolabs. Other reagents (analytical grade) were purchased locally. Hydroxyapatite was prepared in the laboratory (*15*). UDP-glu DH was partially purified from beef liver up to the heat denaturation step where it becomes devoid of associated epimerase activity (*16*). The elution profile of UDP-gal from the reverse-phase (RP) C_{18} μ-Bondapak HPLC column developed with isocratic buffer showed a single sharp peak (details in the text). However, estimation with UDP-glu DH in the presence of NAD, which acts specifically on UDP-glu, showed its occurrence to the extent of 0.3% in UDP-gal (*17*). This was handled at the time of the epimerase assay.

Purification of Epimerase. Unless mentioned otherwise, *K. fragilis* (ATCC-10022 or Microbial Type Culture Collection, Institute of Microbial Technology, Chandigarh, India) was grown in 0.67% YNB (yeast nitrogen base, Hi-media, Bombay, India) containing 1.5% D-(+)-galactose (Sigma) medium (pH 7.2) at 30 °C for 16 h with shaking. Cells were harvested at the early stationary phase when medium diluted 1:9 with water exhibited a turbidity of 0.65 at 650 nm. The enzyme was purified by the classical method of salt fractionation (*12*) involving four major steps: crude cell extraction, two ammonium sulfate fractionations, and subsequent succinate buffer washing. This procedure has limitations such as the inconsistency of the quality of the purity that is achieved, the suspected occasional protease contamination, etc. Therefore, an alternate protocol involving crude cell extraction, 55% ammonium sulfate fractionation, hydroxyapatite treatment, and DEAE-cellulose chromatography was developed (*18*). The preparation after hydroxyapatite treatment was found to be devoid of protease activity with azoalbumin as the substrate. Also, incubation of the purified epimerase under varieties of conditions that favor proteolysis, followed by analysis with SDS−PAGE or Protein-Pak 300 size exclusion (SE)-HPLC, did not show any degradation up to the limits of detection (*4*, *17*). The homogeneity of the epimerase obtained from both the protocols was confirmed by PAGE and SDS−PAGE. The absence of the enzyme·NADH abortive complex in the purified enzyme was evident from an analysis of the bound ligands, which showed the absence of NADH (described in the text). Incomplete recruitment of NAD in the enzyme was ruled out as epimerase, preincubated with 0.05 mM NAD for 15 min prior to the assay, did not exhibit an enhancement of activity. The specific activity of the purified enzyme was 60−70 units/mg in both cases.

Scheme 1: Coupled Assay of Epimerase

$$\text{UDP-gal} \overset{\text{Epimerase}}{\rightleftharpoons} \text{UDP-glu} \xrightarrow{\text{UDP-glu DH + 2 NAD}} \text{UDP-GA} + 2\,\text{NADH} + 2\,\text{H}^+$$

Enzyme Assay. Epimerase activity was measured by a "coupled assay" at 25 °C where conversion of UDP-gal to UDP-glu was continuously monitored at 340 nm by UDP-glu DH and NAD (Scheme 1) (*12*). UDP-glu is converted to UDP-GA with consumption of 2 mol of NAD via UDP-glucose 6-aldehyde as a bound intermediate. This stoichiometry of NAD was taken into consideration while calculating the amount of substrate converted. The assay mixture contained (per milliliter) 0.1 M glycylglycine (pH 8.8), 0.5 mM NAD, 0.1 mM UDP-gal, and 8 units of UDP-glu DH. This was incubated for 10 min to remove contaminating UDP-glu in UDP-gal. The assay was initiated by adding 3−15 nM epimerase. The absorbance change per minute was 0.030 on average, and linear propagation of the conversion of the substrate was observed for at least 8 min. It is important to note that unless preincubation of UDP-gal with UDP-glu DH was carried out, initial enhancement of catalysis was often observed arising from the contaminating impurity of UDP-glu in UDP-gal. The coupling enzyme UDP-glu DH was assayed with UDP-glu as the substrate (*16*). Experiments were performed at 25 °C. One unit of activity has been defined as the amount of enzyme that converted 1 μmol of the substrate per minute at 25 °C.

Kinetic Analysis. The first-order rate constant (k) for the transition from a low to high specific activity of epimerase during the assay was determined using the relation

$$\log \Delta A = \log(A_{obs} - A_{calc}) = \log[(b - a)/k] - kt/2.3$$

where A_{obs} is the measured absorbance at time t, A_{calc} is the absorbance at an early time t obtained by extrapolation of the linear portion of the progress curve, and b and a are the specific activities of the initial and final forms of the enzyme, respectively (*19*). The duration of the lag was obtained from the time axis of the coupled assay by extrapolation of the linear portion of the progress curve. The initial rate of the reaction is defined as the progress up to 30 s obtained from a recording spectrophotometer for which the limit of detection was 0.001. A 10 s gap for manual dispensing and mixing of epimerase for initiation of the assay was uniformly maintained.

In the coupled assay, reaction of the primary enzyme is initiated when the substrate concentration of the auxiliary (coupling) enzyme is zero, leading to a kinetic lag. This lag can be calculated by McClure's analysis (*20*) on the basis of the relation $t = -\{K_M \times 2.303[\log(1 - F_p)]\}/V_2$, where t is the lag time by which the rate of conversion by the coupling enzyme becomes equal to the rate of any desired fraction of the primary enzyme, F_p is the desired fraction of the steady state reaction of the primary enzyme to be measured (a value of 0.99 is reasonably acceptable), and K_M and V_2 are the Michaelis constant of the substrate and the maximum velocity of the coupling enzyme, respectively.

Alternately, the said lag may be predicted with the relationship $t = \Phi K_M/v_1$, where t and K_M are as described above and v_1 is the highest velocity of the primary enzyme (Storer and Cornish-Bowden relation; *21*). A value of Φ is obtained from ref *21* depending on the desired fraction of the steady-state reaction of the primary enzyme to be measured ($v_1/v_2 = 0.99$) and the v_1/V_2 ratio where v_1, v_2, and V_2 represent the velocity of the first and second reactions and the maximum velocity of the second reaction, respectively.

Dissociation, Identification, and Quantification of Nucleotides. Epimerase (1 mL, 10 mg/mL) in 5 mM potassium phosphate (pH 8.0) was heated to 100 °C at 5 °C/min. The elevated temperature was maintained for 5 min, by which point 95% of the protein was precipitated with dissociation of the ligand(s). The supernatant was lyophilized. The released nucleotides were identified as follows. (i) TLC on precoated silica gel 60 F_{254} plates (Merck) was employed using three different solvent systems (50% ethanol, 80% ethanol, and a 40:40:20 isopropyl alcohol/ethanol/water mixture). Nucleotides were viewed under short-wavelength UV radiation. R_f values of standard nucleotides in the three solvent systems were as follows: 0.79, 0.80, and 0.80 for 5′-UMP, 0.86, 0.62, and 0.38 for UDP, 0.77, 0.24, and 0.41 for UTP, 0.80, 0.79, and 0.78 for UDP-man, 0.83, 0.76, and 0.78 for UDP-xyl, 0.88, 0.89, and 0.87 for UDP-GA, and 0.82, 0.57, and 0.56 for heat-treated NAD (0.70 minor). The maximum variation of R_f was ±0.02 ($n = 4-5$). (ii) HPLC by a reverse-phase C_{18} μ-Bondapak column (Waters) using isocratic elution with 10 mM potassium phosphate (pH 7.2) was carried out with a Waters HPLC system and 440 series absorbance detector (*22*). The eluant was monitored at either 254 or 340 nm at a flow rate of 1 mL/min. Since the cofactor(s) of epimerase was dissociated by heating, NAD, NADH, and uridine derivatives used as control were also subjected to heat treatment under identical conditions before analysis. Analyses were carried out with a Shimadzu LC HPLC system with an SPD M10A diode array detector which provided UV absorption spectra of the separated compounds. Retention times and absorption maxima reported (*23*) and observed (within parentheses) of the nucleotides were as follows ($n = 3$): 5.95 min and 260 (260.2) nm for 5′-UMP, 6.20 min and 261 (260.5) nm for UDP, 5.60 min and 260 (260.3) nm for UTP, 5.90 min and 260 (260.5) nm for UDP-man, 6.00 min and 262 (261.7) nm for UDP-xyl, 6.00 min and 262 (262.3) nm for UDP-gal, 6.05 min and 254 (254.5) nm UDP-glu, 5.6 min and 260 (259.9) nm for UDP-GA, 4.5 (minor) and 6.0 min and 260 and 261 (258.2 and 261.2) nm for UDP-NAG, 14.1 min and 258 (257.6) nm for c-AMP, 9.8 min and 253 (253.4) nm for NADH, 2.0 (minor) and 9.8 min (255.5 and 253.4 nm) for heat-treated NADH, 13.8 min and 252 (252.3) nm for NAD, 13.8 min and 252 (252.3) nm for NAD, and 2.0 (minor) and 13.8 min (255.6 and 252.3 nm) for heat-treated NAD. Observed absorption maxima resemble literature values within ±0.5 nm (*23*).

Dissociation of the cofactor and ligands from epimerase by heat treatment involved partial thermal degradation with the possibility of precipitation of the holoenzyme. An alternate approach to dissociate the ligands at ambient temperature was to treat the enzyme with 10% trichloroacetic acid (TCA) or perchloric acid (*24*, *25*). Epimerase was treated with 10% TCA at 25 °C for 10 min, and the supernatant was neutralized to pH 7.0 before fluorimetric estimation of NAD. The cofactor was also estimated fluorimetrically, preventing precipitation of epimerase. The enzyme (1.5−2.0 nmol) in 20 mM potassium phosphate (pH 8.5) was treated with 0.2 M HCl at 25 °C for 30 s to destroy bound NADH, if any. The protein was retained in the solution quantitatively under such acidic conditions because of its low concentration. It was then treated with 6 M NaOH for 1 h when NAD was converted to different fluorescence products (excitation at 360 nm and emission at 460 nm). A linear standard curve was constructed using 0−12 μM NAD against emission intensity under identical alkali treatment (*26*). The amount of bound NAD, after dissociation, was estimated from the calibration curve. In some sets, 3.25 μM NAD was included with the protein as an internal control where the increase in fluorescence intensity was found to be additive. NAD-like compounds also give a fluorescence response after NaOH treatment, but previous studies indicate the absence of such compounds with epimerase (*17*, *27*).

The epimerase was also exposed to 8 M urea at pH 7.0 and 25 °C for 10 min, a point at which the molecule is known to become denatured with dissociation of NAD (*4*, *28*, *29*). A fluorimetric procedure identical to that described above was followed for estimation of the amount of dissociated NAD under denatured conditions against a calibration curve. This curve was constructed with 0−7 μM NAD after NaOH treatment in the presence of 8 M urea. A linear dependence of emission intensity versus NAD concentration was observed (*27*).

Mass Spectrometric Analysis. Epimerase (0.5 mg/mL), was dialyzed extensively against water at 4 °C, lyophilized, and reconstituted in 10 mM potassium phosphate (pH 7.0) at a

concentration of 5 mg/mL. The sample was heat-treated for dissociation of the cofactor and ligand(s) and centrifuged to remove the precipitated protein, and the components in the supernatant were separated by RP-HPLC before application to mass spectral analysis. NAD, uracil sugars, and other derivatives were also heat-treated under identical conditions before application. A Q-Tof micro (Micromass) instrument under positive ionization electrospray mode was used at a desolvation temperature of 200 °C. Argon as a collision gas at 2 kg/cm^2 having a collision energy of 10 ev was applied. Micro channel plate detectors were used.

Enzymatic Analysis. The uridine-like compound that was separated by HPLC from the supernatant of the heat-treated enzyme was diluted 5-fold with 20 mM Tris-HCl (pH 9.0). It was treated with 5 units of 5′-nucleotidase at 37 °C for 8 h to eliminate terminal phosphate groups of nucleotides, if present. Enzymatic conversion was terminated by heating the solution at 100 °C for 5 min before subjecting it to mass spectrometric analysis. Control experiments were carried out with 5′-nucleotidase using 5′-UMP, UDP, and UTP under identical conditions. The 5′-nucleotidase-treated dephosphorylated samples were further phosphorylated with T_4 polynucleotide kinase (PNK). The samples were treated with 0.1 unit of PNK in the same buffer in the presence of 0.5 mM ATP and Mg^{2+} at 37 °C for 2 h. A control experiment was carried out with 0.02 mM uridine and PNK under the same condition. The samples were centrifuged, and the products were analyzed with a mass spectrometer.

NMR Spectroscopy. Epimerase (6.5 mg) was dialyzed exhaustively against glass-distilled water and dried. It was reconstituted in 300 μL of 20 mM sodium phosphate (pH 7.5) and centrifuged to remove the trace amount of turbidity, the final concentration being approximately 20 mg/mL. Its ^{31}P (phosphorus) spectrum was scanned (^{1}H decoupled during acquisition) using a Varian 500 MHz NMR spectrophotometer at 30 °C housed at Bose Institute (Calcutta, India). All spectra were plotted relative to an external standard of 85% phosphoric acid. Inorganic phosphate at pH 7.5 appeared 2 ppm downfield from phosphoric acid. A solution of 5 mM 5′-UMP in the same buffer at pH 7.5 was also scanned for comparison.

Spectroscopic Measurements. The enzyme assay and the UV absorption spectra scan (240−300 nm) were carried out with either a Digispec-200GL UV−vis spectrophotometer or an Analytic Jena Specord 200 recording spectrophotometer attached to a variable-temperature circulating water bath (Polyscience). Fluorescence measurements were carried out with a Hitachi F4020 spectrofluorimeter using a standard 700 μL quartz cuvette. All spectral measurements were taken at 25 °C.

Protein Estimation. The amount of purified epimerase was estimated either with the Bio-Rad Protein Assay dye reagent (Bio-Rad Laboratories, catalog no. 56002) or after Lowry (*30*). In all cases, bovine serum albumin (grade V) served as a reference. Variation of results between the two methodologies was limited to ±10%.

Other Methods. Proteins (100 μL) were separated from extraneous or dissociated ligands by being passed through a prespun (2.9 cm × 0.7 cm) Sephadex G-50 column, usually known as a "spin column", equilibrated with 50 mM potassium phosphate (pH 8.0), and were eluted by low-speed centrifugation. Recovery was 90−95% (*31*). Quantitative retention of small ligands was verified spectrophotometrically or enzymatically by loading strongly absorbing materials or a high concentration of enzyme substrates (*32*). The concentration of nucleotides was determined from extinction coefficients available from the literature. Reversible folding of epimerase (5 mg/mL) was carried out by denaturing with 8 M urea in 20 mM potassium phosphate (pH 7.5) for 10 min at 25 °C when the enzyme unfolded with dissociation of the constituent molecules. Refolding was initiated by 20-fold dilution with the same buffer at 25 °C for 60 min in the presence of 1 mM extraneous NAD. Under such conditions, the holoenzyme structure was reconstituted with an 80−90% restoration of activity (*4*, *28*, *29*).

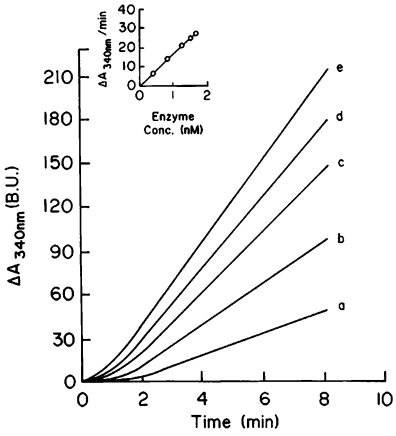

FIGURE 1: Initial time course of the conversion of UDP-gal to UDP-glu by epimerase purified from the late log phase of *K. fragilis* by the coupled assay protocol. Assay conditions have been described in the text. The sets contain the following enzyme concentrations: (a) 0.33, (b) 0.66, (c) 0.99, (d) 1.32, and (e) 1.65 nM. The inset shows the linear dependence of the rate of conversion of UDP-gal to UDP-glu by epimerase at the steady state. The substrate concentration was 0.2 mM, and linearity of the reaction was maintained up to 2 nM epimerase under the defined assay conditions.

RESULTS

Initial Phase of Catalysis. The initial rate of conversion of UDP-gal to UDP-glu by 0.33, 0.66, 0.99, 1.32, and 1.65 nM epimerase as measured by the coupled assay at 25 °C is shown in Figure 1. The durations of the lag of these reactions were 80, 72, 48, 27, and 22 s, respectively, while the ratios of initial versus final rates were 0.0, 0.0, 0.44, 0.50, and 0.64, respectively. These features were not due to insufficient application of the coupling enzyme. The presence of half or double the amount of UDP-glu DH in the assay failed to alter the kinetic parameters (discussed below). The assay produced a linear dependency of rate with enzyme concentration up to 2 nM, beyond which the coupling enzyme became limiting (inset of Figure 1). Thus, every assay reported here was performed at <2 nM epimerase. Analysis of the rate of conversion of epimerase from low to high specific activity or the "activation process" under assay conditions (*19*) showed a linear dependence of log ΔA on time, indicating a first-order reaction. A representative profile with 0.33 nM epimerase has been illustrated in Figure 2A. The rate constants for conversion at 25 °C by the first four enzyme concentrations were 2.12×10^{-2}, 2.30×10^{-2}, 3.22×10^{-2}, and 5.06×10^{-2} s^{-1}, respectively, and the

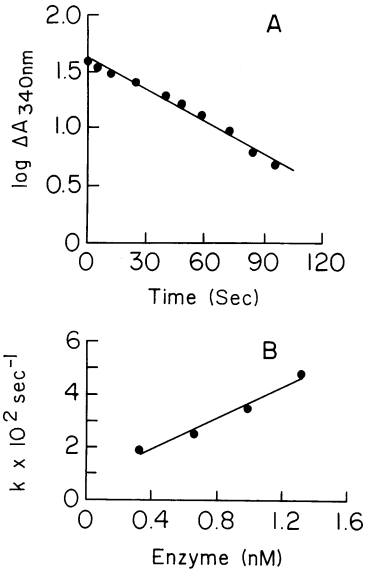

FIGURE 2: Analysis of the rate of conversion of epimerase from low to high specific activity. (A) Dependence of the conversion rate when fitted with first-order kinetics, eq 1 as described in the text. Data were obtained from a recording spectrophotometer representing the reaction of the bottom trace of Figure 1 with 0.33 nM enzyme. The derived k equaled 2.12×10^{-2} s^{-1} at 25 °C. (B) Linear dependence of k on enzyme concentration as obtained from Figure 1.

variation was linear with respect to enzyme concentration (Figure 2B).

The assay with 0.8 nM enzyme between 20 and 40 °C showed an ~4-fold increase in the rate of reaction. The gradual disappearance of the lag from 150 s and the increase in the ratio of the initial rate to final rate from 0 to 1 were complete by 35 °C. Epimerase, preincubated at 40 °C for 10 min followed by cooling to 25 °C for 15 min, however, exhibited a lag similar to the control which was not subjected to such incubation. This showed that mere warming of the enzyme did not alter its kinetic character. Thus, the dependence of the lag on both enzyme concentration and temperature appeared to be inversely related to the catalytic turnover (result not shown).

Lag from the Coupling Enzyme. The lag contributed by UDP-glu DH in the epimerase assay was calculated using the method of McClure (*20*) using a K_m for UDP-glu of 0.013 mM (*16*), an F_p of 0.99, and a V_2 (maximum velocity of the coupling enzyme as applied in the assay protocol) of 6.35 mmol L^{-1} min^{-1}. These led to a t of 0.565 s which was insignificant. Alternately, the lag was calculated after Storer and Cornish-Bowden (*21*) using $t = \Phi K_m/v_1$. When the variation of v_1 between 0.794 and 2.38 mmol L^{-1} min^{-1} and the variation of v_1/v_2 between 0.95 and 0.99 are considered, the derived t varied between 0.442 and 1.19 s. This was once again insignificant and comparable to the McClure calculation.

The validity of these data should be verified from actual experiment (*33*). As mentioned previously (*19*), UDP-glu DH did not exhibit, to the limit of detection, any initial lag in the conversion of UDP-glu under the assay conditions even at the lowest substrate concentration. Also, another form of epimerase, the "clean enzyme" described below, did not exhibit the lag. The assay with 1−1.5 nM epimerase carried out by increasing or decreasing the amount of the coupling enzyme under standard assay conditions showed inhibition of epimerase activity when the coupling enzyme was reduced 10-fold, but an initial lag was observed only when it was further lowered to 50-fold. Similarly, when the level of the coupling enzyme was increased 10-fold, there was no alteration of the parameters. Thus, a safe margin was always maintained to exclude lag arising from the coupling enzyme.

Consideration of Factors Responsible for Lag. Because epimerase is a multimeric enzyme with a cofactor, its kinetic lag may originate from a number of structural phenomena, including "association−dissociation" (*33*−*35*). Epimerase (*K. fragilis*) maintains a stable dimeric structure in 20 mM potassium phosphate (pH 7.5) at 25 °C for months. Dissociation of epimerase in low-salt buffer or in a dilute solution is a day-long process associated with irreversible inactivation (*36*). "Substrate-induced activation" of monomeric epimerase appears to be highly improbable since no gradual enhancement of activity of the clean epimerase during an assay had ever been observed.

To address product activation, the stable end product UDP-GA was generated by treating UDP-glu (0.025 mM) with UDP-glu DH and NAD for 10 h at 25 °C. Complete conversion of UDP-glu was ensured spectrophotometrically by the second addition of UDP-glu DH. UDP-GA so generated, when preincubated with epimerase for 15 min, could not change the lag. Activation due to withdrawal of substrate inhibition did not appear to be feasible as only 1.2% of the substrate was consumed at the initial phase of the assay. Thus, the question of negative cooperativity is not pertinent.

The lag may, however, be a result of the purification procedure in which protein−protein interactions and/or coprecipitation with ligand(s) may take place. An assay with 1 nM epimerase from each step of purification following ref *12* or *18* led to a variation of the initial rate/final rate ratio of 0.425 ± 0.025 or 0.450 ± 0.030 and a duration of the lag of 44 ± 4 or 45 ± 4 s, respectively. To remove any loosely bound inhibitor with the purified enzyme, if any, a 0.25 mg/mL solution of the protein was dialyzed extensively against 0.05 M potassium phosphate (pH 8.5) or passed through a Sephadex G-50 spin column (*30*). Once again, no difference in kinetic parameters could be detected.

As the possibility of activation by proteolysis or partial recruitment of NAD could be excluded, it was necessary to consider that the enzyme might be activated by a substrate-induced minor conformational change on a global scale or at the catalytic site. The former was verified by fluorescence emission analysis of its tyrosine and tryptophan residues in both the presence and absence of 0.025 mM UDP-gal (excitation at 280 nm and emission at 300−450 nm), while the latter was verified by using the extrinsic fluorophore 1-ANS in 200 μM aqueous buffer (excitation at 375 nm and emission at 400−600 nm), which interacts specifically at the substrate-binding site of epimerase (*37*−*39*). The emission spectra were indistinguishable in the two cases, having emission maxima at 338.2 ± 0.2 and 435.5 ± 0.2 nm, respectively.

These experiments collectively suggested that the lag is a true expression of the activity of the epimerase itself, not of an artifact.

Abolition of the Lag. Epimerase (1 nM) was preincubated with its substrates or analogues (1.0 mM) for 10 min at

25 °C and was passed through a Sephadex G-50 spin column. The following results (initial rate/final rate ratio and duration of lag in seconds) were observed: 0.44 and 45 for UMP, 0.44 and 48 for UDP, 0.44 and 42 for UTP, 1.0 and 0 for UDP-gal, 1.0 and 0 for UDP-glu, 0.32 and 60 for D(+)-gal, and 0.35 and 60 for D(+)-glu, respectively. It showed that it was only the substrates that yielded an enzyme incapable of demonstrating the lag, termed the clean enzyme. The prominence of the lag with 0.33 or 0.66 nM enzyme, as illustrated in Figure 1, was absent with an equal concentration of the clean enzyme. The velocities of these reactions at the steady state remained equal to controls without such treatments, indicating their identical turnovers. It was ensured by enzymatic estimation that epimerase preincubated with UDP-gal or UDP-glu was completely devoid of the ligands after passing through the spin column. Recovery of epimerase was, however, 95−97% in terms of activity, indicating retention of enzyme-bound NAD (*29*). Since the spin column requires 2−3 min for separation, the exact dependence of catalytic turnover and abolition of the lag could not be ascertained.

The reversibly reconstituted functional enzyme, after complete denaturation with 8 M urea, also failed to show the lag. If one assumes that the reactivated enzyme has the same specific activity as the native enzyme, the concentration of the reactivated enzyme was calculated on the basis of recovered activity that varied between 80 and 100%. When the assay was performed using 0.046−0.370 nM refolded enzyme, linear propagation of product formation was observed from the onset of the reaction. During previous studies on refolded epimerase, a similar absence of lag was consistently observed (*4*, *26*, *27*).

Analysis of Bound Ligands. The stoichiometry of the bound cofactor(s) of epimerase was determined as follows.

(1) By Fluorescence. Fluorimetric determination of the amount of NAD after 10% TCA precipitation of 2 mg/mL epimerase (1 mL) in comparison with a standard calibration curve yields a stoichiometry of 1.575 residues/dimer (n = 4). An enhancement of the stoichiometry to 1.70 ± 0.1 residues/dimer (n = 5) was observed after alkali treatment using 0.8 nmol of epimerase. In another set, the same quantity of enzyme was pretreated with 8 M urea to ensure complete dissociation of the cofactor. The derived stoichiometry was similar [1.68 ± 0.06 residues/dimer (n = 5)]. The fluorimetric method, however, cannot distinguish between NAD and structurally related nucleotides.

(2) By HPLC. If one assumes that NAD and possibly NADH are associated with epimerase, these nucleotides were treated with heat under conditions identical to those employed to release the ligand(s) from the epimerase. The chromatographic patterns from reverse-phase C_{18} μ-Bonda Pak column of the supernatant of the heat-treated enzyme as well as standard NAD and NADH, both with and without heat treatment, have been described in Figure 3. It shows that NAD was eluted as a major peak in 95% abundance with a retention time (t_R) of 13.8 min, together with a minor contaminant with a t_R of 2.0 min. No absorbance was recorded when the elution was monitored at 340 nm, indicating the absence of NADH in it (result not shown). The elution profile of standard NADH with or without heat treatment was followed at 340 nm. It showed a single peak with a t_R of 9.8 min which is clearly separated from NAD.

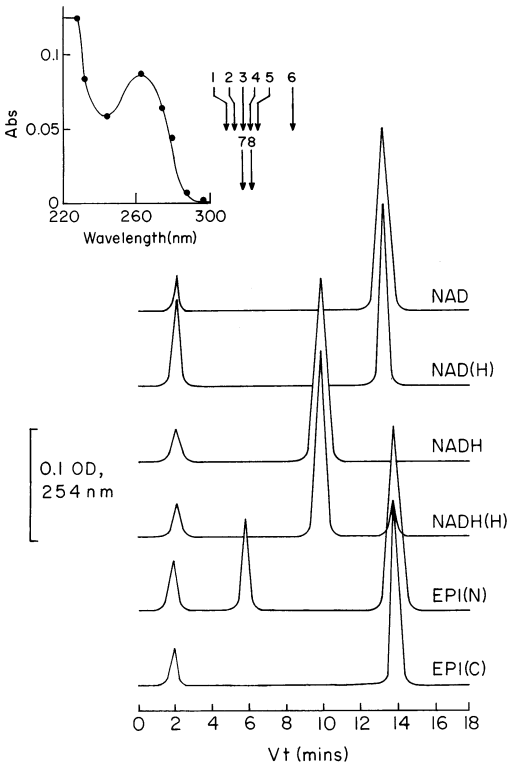

FIGURE 3: Elution profiles of the heat-treated supernatant of epimerase and reference nucleotides from a reverse-phase HPLC column. Detailed experimental conditions have been mentioned in the text. The chromatograms were obtained under isocratic conditions of elution in the presence of 20 mM sodium phosphate buffer (pH 7.0) at a flow rate of 1 mL/min using a C_{18} reverse-phase HPLC column. The elution was monitored at 254 nm. The profiles have been described as follows. NAD and NADH are for the respective nucleotides as available commercially. NAD(H) and NADH(H) are the respective nucleotides after heating at 100 °C for 5 min. EPI(N) represents the supernatant of epimerase obtained after heating under identical conditions, and EPI(C) is the heat-treated supernatant of the same enzyme obtained after undergoing catalysis and passing trough a Sephadex G-50 spin column. The HPLC column was used to run several uracil derivatives as references (marked as 1−8). The retention times and absorption maxima of the compounds that were used have been mentioned in the text. The inset shows UV-absorption spectra between 220 and 300 nm of the compound having a retention time of 5.85 min in the EPI(N) profile. The observed absorption maximum was at 262.3 nm.

However, when the elution was followed at 254 nm, an additional peak was observed with a t_R of 2.0 min which likely is due to an impurity. Because NADH is a thermally stable molecule, its decomposition was not observed to any significant extent.

For estimation of the amount of cofactor(s), 9.6 nmol of enzyme was slowly heat denatured and centrifuged and the supernatant was subjected to HPLC analysis. The profile shows a major peak corresponding to NAD (t_R = 13.8 min) together with another peak with a t_R of 2.0 min which likely is its decomposed product. No NADH associated with epimerase could be detected within the limit of detection of <0.01% relative to NAD. Also, following elution at 340 nm did not reveal any peak. Considering a 15% loss of NAD due to decomposition, 1.3 ± 0.09 mol of NAD per dimer was recovered. What was unexpected was the elution of another component with a t_R of 5.90 ± 0.05 min in considerable abundance. This compound has an UV absorption spectrum typical of a nucleotide having an abs_{max} at

261.0 nm and an $A_{260/280}$ of 1.80 at pH 7.0 (inset of Figure 3). Since uracil derivatives, including uracil sugars, interact specifically at the catalytic site of the enzyme, several such compounds were applied in the HPLC runs for comparison. Their names, retention times, and absorption maxima have already been mentioned in the text. By comparison, the unknown compound apparently comigrated with 5′-UMP or UDP-Man.

(3) By TLC. Attempts were made to separate by TLC nucleotides which had similar retention times as determined by HPLC. Most of them were well separated by silica gel plates as mentioned earlier. In all cases, uracil derivatives and NAD were heat-treated under conditions in which ligands were dissociated from the enzyme. The R_f values of the ligand(s) released from epimerase in solvents A−C were 0.80, 0.80 together with 0.55, and 0.79 together with 0.57, respectively. TLC profiles in combination with HPLC strongly suggested the presence of NAD together with UMP in epimerase. When the HPTLC system (Camag) was used to obtain better resolution, identical results were obtained.

(4) By Mass Spectrometry. The two major peaks (t_R = 5.9 and 13.8 min) from the supernatant of the heat-treated enzyme which appeared in HPLC exhibited the following MS data (FAB): *m*/*z* 325 [$(M + H)^+$] together with *m*/*z* 296, 249, and 665 [$(M + H)^+$]. These corresponded to *m*/*z* 325 [$(M + H)^+$] of 5′-UMP and *m*/*z* 296 and 249 (fragmented products of 5′-UMP) and *m*/*z* 665 [$(M + H)^+$] of NAD. No peaks corresponding to UDP 405, UTP 485, UDP-gal, UDP-glu or UDP-man 611, UDP-xyl 537, UDP-NAG 652, UDP-GA 647, or cAMP 346 were observed. Also, none of these nucleotides yielded fragmented *m*/*z* 296 or 249 products.

(5) By Enzymatic Analysis. The control using 5′-UMP as well as the uridine-like ligand after treatment with 5′-nucleotidase yielded peaks at *m*/*z* 246. If one assumes that 5′-UMP was the ligand, the nucleotidase was expected to yield uridine at (*m*/*z* 246). The dephosphorylated ligand upon PNK treatment yielded peaks at *m*/*z* 325, 405, 485, and 508 which corresponded to 5′-UMP, UDP, UTP, and unreacted ATP, respectively. The dephosphorylated product of 5′-UMP used as a control after PNK treatment yielded identical peaks.

NMR Analysis. ^{31}P NMR offered a convenient way of distinguishing 5′-UMP from other uridine derivatives, uridine sugars, and NAD/NADH as the phosphorus signal appears considerably downfield compared to others and has been successfully applied in analyzing *E. coli* epimerase (*40*, *41*). In the case of *K. fragilis* epimerase, the only singlet peak appeared at a chemical shift (δ) of 1.49 ppm. This may be compared to the signal of 5′-UMP at 0.79 ppm at pH 7.5. The difference is likely to arise from the binding of UMP to the enzyme, leading to an alteration of its pK_a. The absence of any peak upfield up to −10 ppm suggested the absence of other uridine derivatives. Any peak further upfield was not considered assuming that it originated from enzyme-bound NAD.

Taken together, it is indicative that epimerase contains 5′-UMP in addition to NAD. The UMP content of the enzyme was estimated from the HPLC profile after computing area calculation of the eluted peak with respect to a standard 5′-UMP solution run under identical conditions (Figure 3). Correlating with the concentration of the protein, the derived stoichiometry was found to be 0.5 mol/dimer.

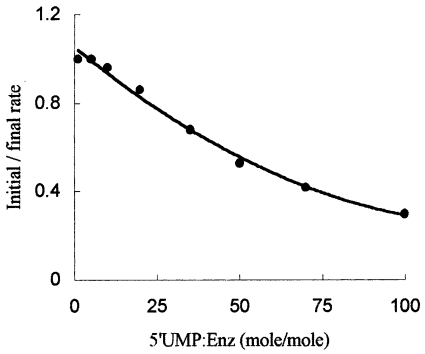

FIGURE 4: Reappearance of kinetic lag in epimerase (clean enzyme) after addition of a molar excess of 5′-UMP. Measurement of initial and final rates has been described in the text, and a ratio of 1 indicates the absence of a lag. The assay was carried out with 1.5 nM epimerase under defined conditions.

Replacement of the Inhibitor with the Substrate. Epimerase that has undergone catalysis (clean enzyme) was found to exhibit no kinetic lag. This enzyme was heat-treated, and the released nucleotides were analyzed by HPLC. The chromatogram showed that NAD and its decomposed products were eluted at identical positions as observed earlier except that the peak of 5′-UMP was completely missing (Figure 3, bottom trace). The substrate UDP-gal or UDP-glu thus must have replaced the inhibitor from epimerase but not the cofactor NAD. Considering the substrate and inhibitor specificity, and also initial suppression of activity and replacement of 5′-UMP during catalysis, it is evident that the ligand was associated at the substrate-binding site of the catalytic domain.

Reappearance of the Lag. It has been demonstrated that when 5′-UMP bound to epimerase was replaced with the substrate, the kinetic lag was removed. A natural progression of this phenomenon was to verify reappearance of the lag by 5′-UMP and its removal by the substrate. The clean enzyme (3 μM) was generated and incubated with a 1−100 fold molar excess of 5′-UMP in 20 mM sodium phosphate (pH 8.0) for 15 min, and aliquots were withdrawn for the assay. The result showed that the lag was continuously prominent; i.e., the initial rate/final rate ratio changed from 1.0 to 0.3 as the excess of the inhibitor was increased from 0 to 50-fold (Figure 4). A further increase in the level of inhibitor to 100-fold did not increase the lag. Inhibition of catalytic activity was observed between 20 and 25% using sets containing a 50−100-fold molar excess of 5′-UMP due to its carry-over to the assay mixture. This experiment was repeated with UDP, UTP, UDP-man, UDP-xyl, UDP-GA, UDP-NAG, and c-AMP. None of them could reintroduce the lag. It may be mentioned that the lag induced by bound UMP and its inhibition on epimerase activity are two independent phenomena, and therefore, different concentrations of UMP were required to produce these effects.

Relation of the Lag to Cell Growth. It is evident that the epimerase purified from *K. fragilis* and harvested at late log phase is associated with an inhibitor suppressing its activity. It is an inducible and essential enzyme for cell growth in the presence of galactose acting as the major carbon source. The epimerase cannot remain inactive during cell growth; thus, it is speculated that it attains the inactive status after a certain stage of cell growth. Two experiments were designed to verify this.

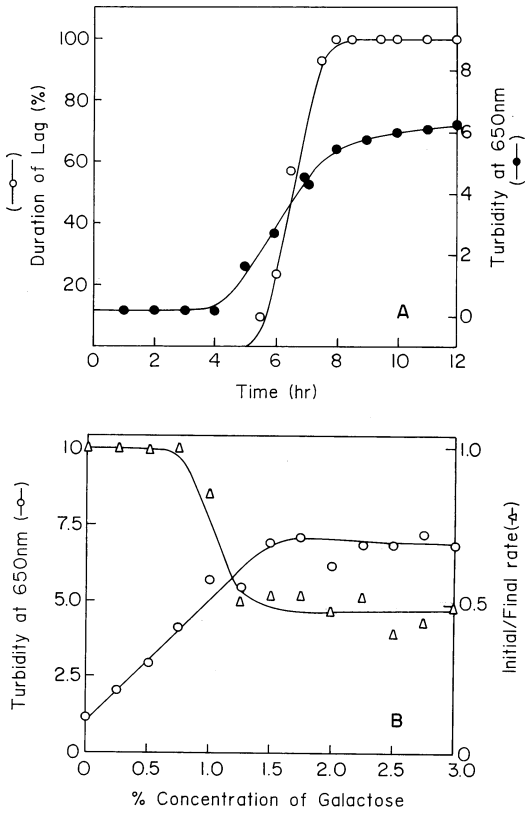

FIGURE 5: Dependence of initial lag of catalysis of epimerase obtained from yeast cells harvested at different intervals of growth or grown at a limiting concentration of galactose. (A) Cells were grown in 1.5% galactose medium for varying time periods, and epimerase was partially purified. The amount of enzyme used in each assay (approximately 0.35 nM) had identical rates of conversion of UDP-gal in the steady state. Up to 4 h, cell growth and hence expression of activity were insignificant. The lag has been expressed as a percentage compared to the maximum observed from epimerase obtained from the late log phase. Cell growth was monitored from turbidity measurement at 650 nm after 10-fold dilution of the medium with water. (B) Dependence of lag, expressed as initial vs final (steady state) rate of catalysis of epimerase obtained from cells grown at different concentrations of galactose for 16 h. Cell growth was monitored as stated above. A value of 1 for the initial rate/final rate ratio indicates the absence of the initial lag. The parameters used to express the lag in panels A and B are similar but inversely related.

Yeast cells were harvested at 1 h intervals, and their growth was estimated from turbidity measurements at 650 nm for a period of 12 h. Cell growth was insignificant up to 4 h and then accelerated exponentially up to 7 h, and then there was very slow growth up to 12 h. From each harvest, epimerase was partially purified up to the hydroxyapatite step. From each set, 0.33 nM enzyme, based on the expressed enzyme activity, was assayed. This quantity of enzyme isolated from the late log phase of cell growth showed a maximum kinetic lag of 80 s (Figure 1, bottom trace). The duration of the lag was estimated by the coupled assay as mentioned earlier and plotted against cell growth (Figure 5A). It was observed that the lag was absent at the initial phase of cell growth up to 5 h but gradually increased from 0 to 90% by 7 h and remained unchanged for an additional 5 h. The results could be reproduced within ±5% ($n = 4$). Thus, it is apparent that as the cells approach maturity epimerase activity is gradually controlled by combination with UMP.

In a different approach, cells were grown with a limiting concentration of galactose, from 0 to 3% (w/w), keeping the conditions constant and the duration of growth at 16 h. Cell growth and expression of epimerase activity were assessed as stated above. As the extent of cell growth was observed to be less than 10%, epimerase activity could not be measured properly till the galactose concentration was above 0.25%. The extent of growth gradually increased from 10 to 70% between 0.25 and 1.5% galactose with an increasing duration of lag as well as a decreasing initial rate/final reaction rate ratio of epimerase formed. Finally, between 1.5 and 3% of galactose cell growth reached a plateau with a constancy of lag as well as the initial rate/final rate ratio of epimerase at 0.5 (Figure 5B). It may be recalled that the duration of lag is inversely related with the initial rate/final rate ratio of conversion. This indicated that during cell growth, when epimerase activity was a necessity, there was no lag in catalysis. But as the termination of growth approached, the lag became prominent, suggesting the *in vivo* inactive status of epimerase.

DISCUSSION

The initial rate of catalysis of epimerase from *K. fragilis*, purified from the late log phase of cell culture by the coupled assay, was so far inconsistent. It had either an initial lag, an enhancement, or the absence of both apparently counteracting each other. Earlier, it was systematically ignored because the assay produced a linear dependence of rate on enzyme concentration as shown in the inset of Figure 1. Subsequently, it was observed that the initial enhancement arose from the presence of UDP-glu, the substrate of the coupling enzyme, in UDP-gal as trace impurity. The kinetic lag shown in Figure 1 was a reproducible phenomenon, provided that the sequence of addition of assay reagents was properly maintained. Analysis of kinetic models describing the lag imparted by UDP-glu DH as a coupling enzyme, supported by actual experimental data, confirmed that its contribution was negligible. After considering a number of factors relevant to the structure and functionality of epimerase, we concluded that it was a true expression of the activity of the enzyme preparation. The phenomenon described here is similar to "hysteresis" and not allostericity. Hysteretic behavior of several monomeric and multimeric enzymes has been reviewed in ref *42*, where experimental artifacts were seriously taken into consideration in arriving at a firm conclusion.

Epimerase that has undergone catalytic turnover or is functionally reconstituted from the unfolded state did not show an initial lag of catalysis, indicating that this was not its constitutional property. Also, an assay at higher temperatures removed the lag. The ligand(s) associated with epimerase capable or incapable of demonstrating the lag was analyzed by HPLC, TLC, UV absorption spectrometry, mass spectrometric analysis, and the ^{31}P NMR profile. The results collectively confirmed the presence of 5′-UMP, a strong competitive inhibitor, was associated with the enzyme. The nucleotide, after dissociation, was dephosphorylated and rephosphorylated with specific enzymes, and analysis of the products by mass spectrometry corroborated the result. Replacement of 5′-UMP with UDP-gal or UDP-glu, which induced catalysis as well, was competitive; the K_i for 5′-UMP was 1.24 mM (*43*, *44*). Apparently, the refolded enzyme was unable to associate with its own dissociating UMP, the final concentration being too low (0.2 μM) to

Table 1: Comparison of Subunit Composition and Stoichiometry of the Bound Cofactor of Class II Oxidoreductases

enzyme	subunit MW	no. of subunits	mol of NAD/mol of enzyme	ref
urocanase				
Pseudomonas putida	61000	2	2	*53*
Trifolium repens	61400	2	nr[a]	*54*
CDP-D-glucose oxidoreductase				
Yersinia pseudotuberculosis	42500	2	requires NAD as a cofactor	*55*
Pseudotuberculosis pseudotuberculosis	45000	2	needs NAD for activity	*56*
S-adenosyl-L-homocysteine hydrolase				
rat liver	47000	4	4	*57, 58*
plant	55000	2/4	nr[a]	*59*
Alcaligenes faecalis	48000	6	6	*59*
Dictyostelium discoideum	47000	4	1 mol of each NAD and NADH	*59*
dehydroquinate synthase				
Aspergillus nidulans	nr[a]	2	nr[a]	*60*
Salmonella typhimurium	38700		nr[a]	*61*
dTDP-D-glucose oxidoreductase				
E. coli	44000	2	2	*62*
Scaharopolyspora erythraea	36000	2	no NAD but requires it	*63*
UDP-galactose 4-epimerase				
bovine mammary gland	40000	1	requires NAD as a cofactor	*64*
E. coli	39000	2	2	*25*
K. fragilis	75000	2	2	this report
myoinositol 1-phosphate synthase				
yeast	62000	4	requires NAD as a cofactor	*65*
ornithine cyclase				
Clostridia	41500	2	1	*2*
UDP-glucuronate decarboxylase				
wheat germ	nr[a]	nr[a]	tightly bound NAD	*2*

[a] Not reported.

inhibit epimerase. Under similar conditions, epimerase also cannot associate with its own dissociating NAD (*4*, *26*). Facile replacement of 5′-UMP with the substrate at elevated temperatures was expected as the situation favored catalytic turnover. The specific role of 5′-UMP in inducing lag was confirmed after its interaction with the clean enzyme. Removal of 5′-UMP by UDP-gal or UDP-glu was associated with removal of the lag and thus reinforced the origin of this phenomenon. The inhibitor bound rather trapped with epimerase was substoichiometric and nondissociable and survived dialysis and precipitation. Once the enzyme had been dissociated and reconstituted, a much higher concentration of 5′-UMP was required to produce the same effect (Figure 4). A similar unusual affinity for NAD has also been observed during *in vivo* synthesis of the enzyme (*1*−*3*). In case of *E. coli* epimerase, structurally related substrate analogues or inhibitors yield stable enzyme−ligand complexes at low temperatures suitable for crystallographic analysis (*45*, *46*).

Epimerase is obliged to remain functional during cell growth in galactose medium. Therefore, the lag originating from reversible inhibition by 5′-UMP is expected to arise only near the end of the growth. This has been experimentally demonstrated using partially purified epimerase isolated from cells grown for varying intervals of time (0−16 h) in galactose medium (Figure 5A). In an alternate approach, the existence of lag was verified when the concentration of galactose in media was limiting, keeping the growth time constant at 16 h. Once again, the lag was not manifested as long as the cells were in the growing phase (Figure 5B). This raises the possibility of biological control of the enzyme inhibiting backward conversion of UDP-glu to UDP-gal when the cell has a sufficient pool of the former. This possibility is supported by the observations that the 5′-UMP level increases in cells as they approach the termination of growth (*47*), and UMP-bound epimerase is resistant to inactivation by proteolysis, inducing stability in the stored enzyme in the cell (*18*).

An important outcome of this study is the speculation about the number of catalytic sites of the enzyme. Quantification of NAD based on its release after direct incubation of the enzyme at 100 °C yielded 1.0 residue/dimer; hence, there must be one catalytic site per dimer as par background literature (*2*, *3*). Coagulation and precipitation were associated processes; this led to the suspicion that the holoenzyme entered into kinetic competition between precipitation and dissociation of NAD. These coupled with partial thermal decomposition, yielding a low stoichiometry for NAD. Quantification of the cofactor was carried out by slow heating to 100 °C from a dilute epimerase solution followed by RP-HPLC. TCA precipitation of epimerase took place at ambient temperature where NAD is dissociated off. Alternately, NAD was dissociated, preventing precipitation. Results show that dissociation of NAD improved the yield to 1.3 ± 0.1 residues/dimer. An alternate fluorimetric protocol without precipitation was subsequently used when the derived stoichiometry improved further to 1.68 ± 0.1. As a supplement, NAD was dissociated by 8 M urea, which ensured the solubility of the enzyme (*4*). With proper controls, the derived stoichiometry reached 1.70 ± 0.15. Considering a 10% variation in protein estimation, this value reached a limit of 1.70 ± 0.32. Thus, the molar ratio of NAD remained consistently approaching 2.0 per dimer. The reasons for the substoichiometric amount of NAD might be limitation of the analytical procedures such as estimation of the amount of protein or NAD or the presence of the apoenzyme in the purified preparation. It is also possible that a fraction of NAD refused to be dissociated even in the presence of 8 M urea since 12−15% of the secondary structure is retained (*4*). Further, epimerase was purified under inducible conditions

Table 2: Amino Acid Sequence of the NAD Binding Region of Oxidoreductases

NAD binding protein	positions of amino acids	sequence	ref
class I			
lactate dehydrogenase (dogfish muscle)	22−38	KITVV**GVGAVG**MACAIS	*60*
alcohol dehydrogenase (horse liver)	194−210	TCAVF**GLGGVG**LSVIMG	*60*
glyceraldehyde-3-phosphate dehydrogenase (rat liver)	3−19	KVGVN**GFGRIG**RLVTRA	*60*
class II			
UDP-galactose 4-epimerase (*E. coli*)	2−19	RVLVTG**GSGYIG**SHTCVQ	*9*
urocanase	169−186	KWILTA**GLGGMG**GAQPLA	*54*
T. repens	187−204	KWVLTA**GLGGMG**GAQA	*58*
P. putida	214−231	KVAVVA**GYGDVG**KGCA	*57*
AdoHcy hydrolase (rat liver)	214−231	KVAVVA**GYGDVG**KGCQS	*57*
D. discoideum	13−30	IVLVTG**GAGYIG**SHTVVE	*58*
UDP-gal 4-epimerase (*S. cerevisiae*)	6−23	ICLVTG**GAGXIG**SHTVVE	*3*

where overexpression could incorporate errors in folding and maturation of the molecule particularly at the catalytic site (*48*, *49*). However, the number of catalytic sites as it stands now is more inclined to two per dimer, similar to that of its *E. coli* counterpart (*8*, *9*).

The stoichiometry of bound 5′-UMP was found to be 0.5 mol/dimer. Assuming that the degrees of dissociation of NAD and 5′-UMP were equally affected during heat treatment, the stoichiometry was modified to 0.65 mol/dimer. With consideration of the 10% variation of protein estimation, it varies between 0.585 and 0.715. The protocol for estimation of the amount of NAD in the presence of 8 M urea without precipitation could not be applied for 5′-UMP because of interference of the denaturant in HPLC. Thus, the stoichiometry might be on the lower side. Therefore, it appeared that there was one site for binding with 5′-UMP per dimer that led to inactivation. The epimerase formed the monomeric apoenzyme after reaction with *p*-chlorobenzoic acid. Reconstitution of the fully functional holoenzyme after treatment with radioactive NAD and DTT also indicated incorporation of one NAD per dimer (*5*). Thus, it remains speculative that out of two NAD binding sites, presumably catalytic sites, too, only one is functional.

At this point, it is worth considering the stoichiometry of bound NAD in other class II oxidoreductases. The molecular weight, subunit composition, and NAD content of eighteen such enzymes having nine different specificities have been summarized in Table 1. Of these, the stoichiometries of bound NAD of only seven enzymes have been reported, though some enzymes require extraneous NAD as a cofactor. The compilation shows that except for ornithine cyclase, the stoichiometry of NAD (or NADH) stands to be one per subunit, similar to that reported for *E. coli* (*8*, *9*) and yeast epimerase (this report).

X-ray crystallographic structure analysis shows that a conserved double $\beta\alpha\beta\alpha\beta$ motif is a common structural feature of many enzymes that bind NAD and related cofactors (*50*). In proteins where NAD binding sites have been sequenced, it has been possible to define a "fingerprint" characteristic of the dinucleotide-binding domains even in the absence of stringent sequence homology. This domain as defined by Wierenga and Hol (*51*) consists of a $\beta\alpha\beta$ motif with the following features: the GXGXXG sequence in the region joining the first β-strand and the N-terminus of the α-helix, the presence of a hydrophilic residue at the beginning of the first β-sheet region, and the presence of an acidic residue at the C-terminus of the second β-sheet. The amino acid sequence around the fingerprint region of three class I oxidoreductases and five class II enzymes is given in Table 2. It clearly shows that each subunit of class II enzymes, the sequences of which are known, has an independent and defined NAD binding motif.

So far, it has not been possible to design an experiment compatible with *K. fragilis* epimerase that can identify the location of its catalytic sites, i.e., whether at the subunit interface or away from it as in its bacterial counterpart (*52*). Specific modification reactions currently being undertaken are expected to yield a confirmatory answer to this question (A. Brahma and D. Bhattacharyya, unpublished results). However, association of 1 mol of 5′-UMP/dimer leading to complete inactivation suggests the existence of one functional catalytic site.

ACKNOWLEDGMENT

We are grateful to M/s Anchrom (Bombay, India) for offering HPTLC analysis at their Bombay office, Mr. Barun Mazumder and Prof. Siddhartha Roy (Bose Institute) for NMR analysis, Drs. Ranjan Bhadra and Samir K Mondal [Indian Institute of Chemical Biology (IICB)] for use of the Shimadzu HPLC instrument, Mr. Kalyan Sarkar (IICB) for mass spectrometric analysis, and Dr. Basudeb Achariya (IICB) for critical reading of the manuscript.

REFERENCES

1. Gabrial, O., Kalckar, H. M., and Darrow, R. A. (1975) UDP-galactose 4-epimerase, in *Subunit Enzymes: Biochemistry and Function* (Ebner, K. B., Ed.) pp 85−133, Marcel Dekker, New York.
2. Frey, P. A. (1987) Complex pyridine nucleotide dependent transformations, in *Pyridine Nucleotide Coenzymes: Chemical, Biochemical and Medical Aspects* (Dolphin, D., Poulson, R., and Avarmovie, O., Eds.) Vol. 2B, pp 447−462, Wiley, New York.
3. Frey, P. A. (1996) The Leloir pathway: a mechanistic imperative for three enzymes to change the stereochemical configuration of a single carbon in galactose, *FASEB J. 10*, 461−470.
4. Bhattacharyya, D. (1993*)* Reversible folding of UDP-galactose 4-epimerase from yeast *Kluyveromyces fragilis*, *Biochemistry 32*, 9726−9734.
5. Majumdar, S., Bhattacharjee, H., Bhattacharyya, D., and Bhaduri, A. (1998*)* UDP-galactose-4-epimerase from *Kluyveromyces fragilis*: Reconstitution of holoenzyme structure after dissociation with parachloromercuribenzoate, *Eur. J. Biochem. 257*, 427−433.
6. Bhattacharjee, H., and Bhaduri, A. (1992) Distinct functional roles of two active site thiols in UDP-glucose 4-epimerase from *K. fragilis*, *J. Biol. Chem. 267*, 11714−11720.
7. Webster, T. D., and Dickson, R. C. (1988) Nucleotide sequence of the galactose gene cluster of *Kluyveromyces lactis*, *Nucleic Acids Res. 16*, 8192−8194.

8. Bauer, A. J., Rayment, I., Frey, P. A., and Holden, H. M. (1992) The molecular structure of UDP-galactose 4-epimerase from *Escherichia coli* determined at 2.5 Å resolution, *Proteins: Struct., Funct., Genet. 12*, 372−381.
9. Thoden, J. B., Frey, P. A., and Holden, H. M. (1996) Molecular structure of the NADH/UDP-glucose abortive complex of UDP-galactose 4-epimerase from *E. coli*: Implication for the catalytic mechanism, *Biochemistry 35*, 5137−5144.
10. Kalckar, H. M., Bertland, A. U., II, and Bugge, B. (1970) The reductive inactivation by UDP-galactose 4-epimerase from yeast and *E. coli*, *Proc. Natl. Acad. Sci. U.S.A. 65*, 1113−1119.
11. Thoden, J. B., Wohlers, T. M., Frodovich-Keil, J. L., and Holden, H. M. (2000) Crystallographic evidence for Tyr 157 functioning as the active site base in human UDP-galactose 4-epimerase, *Biochemistry 39*, 5691−5701.
12. Darrow, R. A., and Rodstrom, R. (1968) Purification and properties of uridine diphosphate galactose 4-epimerase from yeast, *Biochemistry 7*, 1645−1654.
13. Datta, S., Maity, N. R., and Bhattacharyya, D. (1997) Reversible folding of UDP-galactose 4-epimerase from *E. coli*, *Eur. J. Biochem. 244*, 407−413.
14. Barat, B., and Bhattacharyya, D. (2001) UDP-galactose 4-epimerase from *Escherichia coli*: Formation of catalytic site during reversible folding, *Arch. Biochem. Biophys. 391*, 188−196.
15. Bernardi, G. (1971) Chromatography of nucleic acids on hydroxyapatite columns, *Methods Enzymol. 21*, 95−147.
16. Zalitis, J., Uram, M., Bowser, A. M., and Feingold, D. S. (1972) UDP-glucose dehydrogenase from beef liver, *Methods Enzymol. 28*, 430−435.
17. Nayar, S. (2000) Studies on the subunit structure and folding behaviour of a complex multimeric enzyme: UDP-galactose 4-epimerase, Ph.D. Thesis, Jadavpur University, Calcutta, India.
18. Brahma, A., and Bhattacharyya, D. (2004) UDP-galactose 4-epimerase from *Kluyveromyces fragilis*: Evidence for independent mutarotaion site, *Eur. J. Biochem. 271*, 58−68.
19. Dalziel, K., McFerran, N., Matthews, B., and Reynolds, C. H. (1978) Transient kinetics of nicotinamide-adenine dinucleotide phosphate linked isocitrate, *Biochem. J. 171*, 743−750.
20. McClure, W. R. (1969) A kinetic analysis of coupled enzyme assays, *Biochemistry 8*, 2782−2786.
21. Storer, A., and Cornish-Bowden, A. (1974) The kinetics of coupled enzyme reaction: applications to the assay of glucokinase with glucose 6-phosphate dehydrogenase as coupling enzyme, *Biochem. J. 141*, 205−209.
22. Newton, J. C., Faynor, M. S., and Northrop, B. D. (1983) Purification of reduced NAD by ion-exchange and high performance liquid chromatography, *Anal. Biochem. 132*, 50−53.
23. *Handbook of Biochemistry: Selected data for Molecular Biology*, 2nd ed. (1973) Section G, pp G-1−G-238, CRC Press, Boca Raton, FL.
24. Liu, Y., Vanhooke, J. L., and Frey, P. A. (1996) UDP-galactose 4-epimerase: NAD content and a charge-transfer band associated with the substrate-induced conformational transition, *Biochemistry 35*, 7615−7620.
25. Wilson, D. B., and Hogness, D. S. (1964) The enzymes of the galactose operon in *Escherichia coli* I. Purification and characterization of uridine diphophogalactose 4-epimerase, *J. Biol. Chem. 248*, 33−40.
26. Udenfriend, S. (1962) Vitamins, coenzymes and their metabolites, in *Fluorescence assay in biology and medicine*, Vol. 1, p 249, Academic Press, New York.
27. Barat, B. (1999) Architecture and refolding of a complex multimeric protein: UDP-galactose 4-epimerase, Ph.D. Thesis, Jadavpur University, Calcutta, India.
28. Dutta, S., Maity, N. R., and Bhattacharyya, D. (1997) Multiple unfolded states of UDP-galactose 4-epimerase from yeast *K. fragilis*: involvement of proline cis−trans isomerisation in reactivation, *Biochim. Biophys. Acta 1343*, 251−262.
29. Maity, N. R., Barat, B., and Bhattacharyya, D. (1999) UDP-galactose 4-epimerase from *Kluyveromyces fragilis*: Equilibrium unfolding studies, *Indian J. Biochem. Biophys. 36*, 433−441.
30. Lowry, O. H., Rosenbrough, N. J., Farr, A. L., and Randall, R. J. (1951) Protein measurement with the folin-phenol reagent, *J. Biol. Chem. 193*, 265−276.
31. Maniatis, T., Fritsh, E. F., and Sambrook, J. (1982) Biochemical Techniques, in *Molecular Cloning: A Laboratory Manual*, pp 466−467, Cold Spring Harbor Laboratory Press, Plainview, NY.
32. Nath, S., Brahma, A., and Bhattacharyya, D. (2003) Extended application of gel-permeation chromatography by spin column, *Anal. Biochem. 320*, 199−206.
33. Rudolph, F. B., Baugher, B. W., and Beissner, R. S. (1979) Techniques in coupled enzyme assays, *Methods Enzymol. 63*, 22−42.
34. Traut, T. W. (1994) Dissociation of enzyme oligomers: A mechanism for allosteric regulation, *Crit. Rev. Biochem. Mol. Biol. 29*, 125−163.
35. Jaenicke, R. (1991) Protein stability and molecular adaptation to extreme conditions, *Eur. J. Biochem. 202*, 715−728.
36. Darrow, R. A., and Rodstrom, R. (1970) Uridine diphosphate galactose-4-epimerase from yeast: Studies on the relationship between quaternary structure and catalytic activity, *J. Biol. Chem. 245*, 2036−2042.
37. Samanta, A. K., and Bhaduri, A. (1982) Interaction of 8-anilino 1-naphthalene sulphonic acid with UDP-glucose 4-epimerase from *Saccharomyces fragilis*, *Indian J. Biochem. Biophys. 19*, 320−323.
38. Samanta, A. K., and Bhaduri, A. (1983) Characterization of pyridine nucleotide binding site of UDP-glucose 4-epimerase from *Saccharomyces fragilis*, *J. Biol. Chem. 258*, 11118−11122.
39. Ray, S., Mukherji, S., and Bhaduri, A. (1995) Two tryptophans at the active site of UDP-glucose 4-epimerase from *Kluyveromyces fragilis*, *J. Biol. Chem. 270*, 11383−11390.
40. Konopka, J. M., Halkides, C. J., Vanhooke, J. L., Gorenstein, D. G., and Frey, P. A. (1989) UDP-galactose 4-epimerase: Phosphorous-31 nuclear magnetic resonance analysis of NAD and NADH bound at the active site, *Biochemistry 28*, 2645−2654.
41. Vanhooke, J. L., and Frey, P. A. (1994) Characterization and activation of naturally occurring abortive complexes of UDP-galactose 4-epimerase from *E. coli*, *J. Biol. Chem. 269*, 31496−31504.
42. Neet, K., and Ainslie, G. R., Jr. (1980) Hysteretic enzymes, *Methods Enzymol. 64*, 192−226.
43. Davis, J. E., Nolan, L. D., and Frey, P. A. (1974) UMP-dependent reduction of UDP-galactose 4-epimerase-NAD^+ complex by sodium cyanoborohydride, *Biochim. Biophys. Acta 334*, 442−447.
44. Kang, U. G., Nolan, L. D., and Frey, P. A. (1975) Uridine diphosphate galactose 4-epimerase. Uridine monophosphate dependent reduction by α- and β-D-glucose, *J. Biol. Chem. 250*, 7099−7105.
45. Thoden, J. B., Frey, P. A., and Holden, H. M. (1996) High-resolution X-ray structure of UDP-galactose 4-epimerase complexed with UDP-phenol, *Protein Sci. 5*, 2149−2161.
46. Thoden, J. B., Frey, P. A., and Holden, H. M. (1996) Crystal structure of oxidised and reduced forms of UDP-galactose 4-epimerase isolated from *E. coli*, *Biochemistry 35*, 2557−2566.
47. Sergio, T. E., and Helenius, A. (1999) Glycoprotein reglucosylation and nucleotide sugar utilization in the secretory pathway: identification of a nucleoside diphosphatase in the endoplasmic reticulum, *EMBO J. 18*, 3282−3292.
48. Bradley, M. K. (1990) Overexpression of proteins in eukaryotes, *Methods Enzymol. 182*, 112−132.
49. Jaenicke, R., and Rudolph, R. (1986) Refolding and association of oligomeric proteins, *Methods Enzymol. 131*, 218−250.
50. Lesk, A. M. (1995) NAD-binding domains of dehydrogenases, *Curr. Opin. Struct. Biol. 5*, 775−783.
51. Wierenga, R. K., and Hol, W. G. J. (1983) Predicted nucleotide-binding properties of p21 protein and its cancer-associated variant, *Nature 302*, 842−844.
52. Nayar, S., and Bhattacharyya, D. (1997) UDP-galactose 4-epimerase from *E. coli:* Existence of a catalytic monomer, *FEBS Lett. 409*, 449−451.
53. Koberstaedt, A., Lenz, M., and Retey, J. (1992) Isolation, sequencing and expression in *E. coli* of the urocanase gene from white clover (*Trifolium repens*), *FEBS Lett. 311*, 206−208.
54. Retey, J. (1994) The urocanase story: A novel role of NAD^+ as electrophile, *Arch. Biochem. Biophys. 268*, 1−8.
55. Yu, Y., Russell, R. N., Thorson, J. S., Liu, L., and Liu, H. (1992) Mechanistic studies of the biosynthesis of 3,6-dideoxyhexoses in *Yersinia pseudotuberculosis.* Purification and stereochemical analysis of CDP-D-glucose oxidoreductase, *J. Biol. Chem. 267*, 5868−5875.
56. Gonzalez-Porque, P., and Strominger, J. L. (1972) Enzymatic synthesis of cytidine diphosphate 3,6-dideoxyhexoses. VI. Purification to homogeneity and some properties of cytidine diphosphate-D-glucose oxidoreductase, enzyme E_1 and enzyme E_3, *J. Biol. Chem. 247*, 6748−6756.

57. Richards, H. H., Chiang, P. K., and Cantoni, G. L. (1978) Adenosylhomocysteine hydrolase: Crystallisation of the purified enzyme and its properties, *J. Biol. Chem. 253*, 4476−4480.
58. Gomi, T., Ishiguro, Y., and Fujioka, M. (1985) *S*-Adenosylhomocysteinase from rat liver. Evidence for structurally identical and catalytically equivalent subunits, *J. Biol. Chem. 260*, 2789−2793.
59. Hohman, R. J., Guitton, M. C., and Veron, M. (1985) Inactivation of *S*-adenosyl-L-homocysteine hydrolase by cAMP results from dissociation of enzyme-bound NAD^+, *Proc. Natl. Acad. Sci. U.S.A. 82*, 4578−4581.
60. Carpenter, E. P., Hawkins, A. R., Frost, J. W., and Brown, K. A. (1998) Structure of dehydroquinate synthase reveals an active site capable of multistep catalysis, *Nature 394*, 299−302.
61. Bentley, R. (1990) The shikimate pathway: a metabolic tree with many branches, *Crit. Rev. Biochem. Mol. Biol. 25*, 307−384.
62. Wang, S.-F., and Gabriel, O. (1969) Biological mechanisms involved in the formation of deoxy sugars, *J. Biol. Chem. 244*, 3430−3437.
63. Vara, J. S., and Hutchinson, C. R. (1988) Purification of thymidine-diphospho-D-glucose 4,6-dehydratase from an erythromycine-producing strain of *Scaharopolyspora erythraea* by high-resolution liquid chromatography, *J. Biol. Chem. 263*, 14992−14995.
64. Geren, C. R., and Ebner, K. E. (1977) Purification and characterization of UDP-galactose 4-epimerase from bovine tissues, *J. Biol. Chem. 252*, 2082−2088.
65. Donahue, T. F., and Henry, S. A. (1981) Myo-inositol 1-phosphate synthase. Characteristic of the enzyme and identification of its structural gene in yeast, *J. Biol. Chem. 256*, 7077−7085.

BI049569T